

Pressure Effects on Superconducting Properties of a BiS₂-based Superconductor Bi₂(O,F)S₂

Tomoyuki Okada¹, Hiraku Ogino^{1*}, Jun-ichi Shimoyama¹, Kohji Kishio¹, Nao Takeshita², Naoki Shirakawa², Akira Iyo² and Hiroshi Eisaki²

¹ Department of Applied Chemistry, The University of Tokyo, 7-3-1 Hongo, Bunkyo-ku, Tokyo, 113-8656, Japan

². National Institute of Advanced Industrial Science and Technology, 1-1-1 Umezono, Tsukuba, Ibaraki, 305-8658, Japan

Pressure effects on a recently discovered BiS₂-based superconductor Bi₂(O,F)S₂ ($T_c = 5.1$ K) were examined via two different methods; high pressure resistivity measurement and high pressure annealing. The effects of these two methods on the superconducting properties of Bi₂(O,F)S₂ were significantly different although in both methods hydrostatic pressure is applied to the sample by the cubic-anvil-type apparatus. In high pressure resistivity measurement, T_c linearly decreased at the rate of -1.2 K GPa⁻¹. In contrast, the T_c of 5.1 K is maintained after high pressure annealing under 2 GPa and 470°C of optimally doped sample despite significant change of lattice parameters. In addition, superconductivity was observed in fluorine-free Bi₂OS₂ after high pressure annealing. These results suggest that high pressure annealing would cause a unique effect on physical properties of layered compounds.

1. Introduction

Since the discovery of superconductivity in Bi₄O₄S₃¹⁾, various layered superconductors with rock-salt type BiS₂ layer have been reported. BiS₂-based superconductors have varied blocking layers such as fluorite-type RE(O,F) layer (RE = La², Ce³, Pr⁴ and Nd⁵) and (Sr,La)F layer⁶). Recently some related compounds with complex stacked structure, such as Eu₃Bi₂S₄F₄ ($T_c = 1.5$ K)⁷⁾ and LaPbBiS₃O (non-superconductor)⁸⁾, has also been reported.

Some of the BiS₂-based superconductors show increase of T_c by applying high pressures (HP). In HP resistivity measurement, La(O,F)BiS₂ shows sudden increase of T_c at ~1 GPa from ~3 K to ~10 K⁹⁾ and then T_c slowly decreases at the slope of -0.28 K GPa⁻¹¹⁰⁾. Structural analysis at room temperature suggests that structural phase transition from

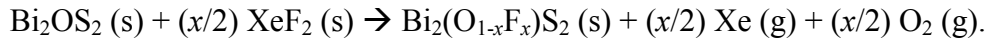
tetragonal ($P4/nmm$) to monoclinic ($P2_1/m$) structure would be responsible for the increase of T_c ¹⁰⁾. Other $RE(O,F)BiS_2$ ($RE = Ce \sim Nd$)^{9,11)}, $(Sr,La)FBiS_2$ ¹²⁾, and $Eu_3Bi_2S_4F_4$ ¹³⁾ also shows the jump-up of T_c to 7~10 K at a certain pressure of 1~2 GPa.

Similar increase of T_c is also obtained by “HP annealing”. In HP annealing, the as-synthesized samples undergo heat treatment in HP synthesis apparatus and physical properties are measured under ambient pressure. In $La(O,F)BiS_2$, T_c increase from ~3 K to 10.6 K after HP annealing at 2 GPa, 600°C²⁾. $Ce(O,F)BiS_2$ ¹⁴⁾ and $Pr(O,F)BiS_2$ ¹⁵⁾ also show increase of T_c by HP annealing. In HP annealing, crystal structure is kept at tetragonal and uniaxial contraction of the lattice along c -axis is attributed to the cause for the increase of T_c ^{15,16)}.

Recently, superconductivity in $Bi_2(O,F)S_2$ (i.e. $Bi(O,F)BiS_2$), which is isostructural with $RE(O,F)BiS_2$, is reported¹⁷⁾¹⁸⁾. T_c varies with changing F-doping level in the underdoped region and reaches to 5.1 K in the optimally-doped sample, while it is impossible to obtain overdoped sample due to the solubility limit of F⁻ for the O²⁻ site¹⁷⁾. In the present paper, pressure effects on $Bi_2(O,F)S_2$ were examined by HP resistivity measurement and HP annealing. The difference of these two methods in the variation of T_c in $Bi_2(O,F)S_2$ is discussed.

2. Experimental

Undoped Bi_2OS_2 was synthesized via solid-state reaction at 300°C, ~100 h in an evacuated quartz ampule with several intermediate grindings. $Bi_2(O,F)S_2$ was synthesized by the topotactic reaction between undoped Bi_2OS_2 and XeF_2 at 400°C, 72 h in an evacuated quartz ampule according to the following chemical reaction.



$Bi_2(O,F)S_2$ samples with different F-content were separately prepared by changing the nominal amount of XeF_2 between $(x/2) = 0.1\sim0.5$. Note that actual composition of F is supposed to be smaller than the nominal x , while investigation of actual F content is difficult due to the small difference in X-ray scattering factors between O and F. Details of synthesis procedure are described in ref 17).

Resistivity measurements were performed by the four-probe method both in ambient pressure and under HP. Resistivity at ambient pressure is measured by Quantun Design Physical Property Measurement System (PPMS). In HP resistivity measurement, hydrostatic pressures up to 11 GPa were applied to the Teflon sample cell together with liquid pressure-transmitting medium Daphne oil 7474 in a cubic-anvil-type apparatus¹⁹⁾.

HP annealing was performed on the as-synthesized Bi_2OS_2 and $Bi_2(O,F)S_2$ at 300~470°C, 2 GPa for 1 h in a cubic-anvil-type apparatus. HP synthesis of Bi_2OS_2 was also performed from Bi_2O_3 (Furuuchi Chemical, 99.9%) and Bi_2S_3 (ALDRICH, 99%) powders at 300~550°C, 2~4 GPa. BN was used for the pressure media. The constituent phases of the samples were

analyzed by X-ray diffraction (XRD) measurement (RIGAKU Ultima-IV) with Cu- K_{α} radiation generated at 40 kV and 40 mA. Silicon powder was used as an internal standard to determine the lattice parameters. Magnetization measurements were performed by a superconducting quantum interference device (SQUID) magnetometer (Quantum Design MPMS) and some measurements were performed down to 0.47 K using iHelium3²⁰⁾.

3. Results

3.1 High pressure resistivity measurement on $\text{Bi}_2(\text{O},\text{F})\text{S}_2$

Hydrostatic high pressure resistivity measurement is performed for the optimally-doped $\text{Bi}_2(\text{O},\text{F})\text{S}_2$ polycrystalline bulk sample with $T_c = 5.1$ K. The temperature dependence of resistivity under pressures of 0~11 GPa is shown in **Fig. 1**. T_c monotonically decreases by application of hydrostatic pressure of 1~2 GPa. At 2 GPa, T_c^{onset} was decreased to 2.7 K and zero resistivity was not observed above 2.5 K. The slope for the almost linear decrease of T_c with applying pressure is calculated to be -1.2 K GPa⁻¹ as shown in **Fig. 2**. The superconducting transition remain sharp even under high pressures, with $\Delta T_c \sim 0.4$ K, suggesting that high pressure is homogeneously applied to the bulk sample.

Under higher pressures than 2 GPa, superconductivity is disappeared. Instead, two other anomalies, marked T_{a1} and T_{a2} in **Fig. 1**, are observed. Origins of these anomalies are attributed to the superconductivity of Bi metal under high pressures. As shown in **Fig. 3(a)**, our sample contains small amount of Bi metal as an impurity phase. The ambient pressure phase of Bi metal, trigonal Bi(I), is not a superconductor. High pressures induce several steps of structural transitions to so-called Bi(II), Bi(III) and Bi(V) phases. Orthorhombic Bi(III) and bcc Bi(V) phases exhibit superconductivity and T_{cs} of Bi(III)²¹⁾ and Bi(V)²²⁾ are very close to T_{a1} and T_{a2} , respectively, as shown in **Fig. 2**.

The sudden increase of T_c at a certain pressure observed in $RE(\text{O},\text{F})\text{BiS}_2$ ($RE = \text{La} \sim \text{Nd}$)^{9,11)}, $(\text{Sr},\text{La})\text{FBiS}_2$ ¹²⁾, and $\text{Eu}_3\text{Bi}_2\text{S}_4\text{F}_4$ ¹³⁾ was not observed in $\text{Bi}_2(\text{O},\text{F})\text{S}_2$. The decrease of T_c with applying pressure is rather similar to the case of $\text{Bi}_4\text{O}_4\text{S}_3$ ²³⁾ or $\text{Bi}_3\text{O}_2\text{S}_3$ ²⁴⁾. We note that crystal structure of $\text{Bi}_4\text{O}_4\text{S}_3$ and $\text{Bi}_3\text{O}_2\text{S}_3$ phase is still controversial²⁵⁾, but both structure contains fluorite-type BiO layer in the blocking layer, as $\text{Bi}_2(\text{O},\text{F})\text{S}_2$ does.

3.2 High pressure annealing on $\text{Bi}_2(\text{O},\text{F})\text{S}_2$

High pressure (HP) annealing was performed for the as-synthesized $\text{Bi}_2(\text{O},\text{F})\text{S}_2$ with different F-content. Here we discuss the effects of HP annealing on two types of samples; underdoped sample with $T_c = 3.0$ K, and optimally-doped sample with $T_c = 5.1$ K.

Figure 3(a) shows powder XRD patterns of $\text{Bi}_2(\text{O},\text{F})\text{S}_2$ samples before and after HP annealing at 470°C and 2 GPa for 1 h. After HP annealing, constituent phases were almost unchanged and the peaks for $\text{Bi}_2(\text{O},\text{F})\text{S}_2$ were well indexed to the space group $P4/nmm$ as well as the as-synthesized samples. a -axis length and c -axis length slightly increased and

largely decreased, respectively, suggesting uniaxial contraction of the lattice along the c -axis as in the case of La(O,F)BiS₂¹⁶⁾ and Pr(O,F)BiS₂¹⁵⁾. We note that the full width at half maximum (FWHM) of the XRD peaks were broadened after HP annealing, suggesting introduction of lattice strain.

The Zero-Field-Cooled (ZFC) magnetizations of these samples are shown in **Fig. 3(b)**. In the underdoped sample with $T_c = 3.0$ K, T_c increased to 4.5 K after HP annealing. Assuming that F-content of the sample is not changed by HP annealing, the uniaxial contraction of the lattice discussed above is supposed to be responsible for the increase of T_c .

In contrast, in the optimally-doped sample with $T_c = 5.1$ K, T_c almost unchanged even after HP annealing despite significant change of lattice parameters. The ZFC curve of the HP annealed sample seems to be somewhat shifted to lower temperatures. However, the onset of diamagnetic transition is kept at 5.1 K and perfect diamagnetism is achieved even at slightly higher temperature, indicating sharpening of the superconducting transition by HP annealing. The maintenance of T_c at 5.1 K is rather similar to the case of Nd(O,F)BiS₂, which also maintains T_c of ~5 K before and after HP annealing²⁶⁾, than the case of RE(O,F)BiS₂ with RE = La~Pr where T_c is increased by HP annealing^{2,15,16)}. Here it should be noted again that T_c^{onset} of optimally-doped Bi₂(O,F)S₂ at 2 GPa was 2.7 K in HP resistivity measurement, significantly lower than that of the same sample annealed at 2 GPa. In HP annealing, high pressure is applied at high temperatures and physical properties are measured at ambient pressure. The difference of these two methods should not be dismissed.

3.3 Superconductivity of high pressure annealed / synthesized Bi₂OS₂

HP annealing is also performed for undoped Bi₂OS₂ synthesized under ambient pressure. As shown in **Fig. 4(a)**, the constituent phases were almost unchanged, and a - and c -axis length increased and decreased, respectively, as in the case of F-doped to Bi₂OS₂.

As-synthesized Bi₂OS₂ did not show large diamagnetism due to superconductivity above 0.47 K. We note that the magnetization curve for as-synthesized Bi₂OS₂ shown in **Fig. 4(b)** is obtained at 200 Oe, because at low field, dipole like waveform was not obtained at 0.47 K and it was impossible to carry out precise measurement. This apparently indicates that as-synthesized undoped Bi₂OS₂ is not a superconductor above 0.47 K.

In contrast, HP annealed Bi₂OS₂ showed superconductivity. The onset of diamagnetic transition is ~4 K, a kink in ZFC curve is at 1.8 K and large diamagnetism is observed below this temperature. HP synthesis was also tried to obtain Bi₂OS₂ from Bi₂O₃ and Bi₂S₃ at 470°C, 2 GPa for 1 h. Bi₂OS₂ was obtained as the main phase while the amount of impurity phases increased compared to HP annealed samples. Lattice parameters and magnetization of the HP synthesized Bi₂OS₂ were almost equivalent to those of HP annealed sample. This sample showed small diamagnetism from ~4 K and large diamagnetism is achieved below 2.1 K, as shown in the inset of **Fig. 4(b)**. These results suggest that the T_c of bulk

superconductivity for the HP annealed / synthesized samples are \sim 2 K. The transition at \sim 4 K is probably due to a impurity phase with small amount such as $\text{Bi}_3\text{O}_2\text{S}_3$, although it is not seen in the XRD pattern.

4. Discussion

Figure 5(a) shows the T_{c} s at ambient pressure and at \sim 2 GPa for various BiS_2 -based superconductors reported to date as a function of a -axis length. The values of a -axis lengths are measured at room temperature and ambient pressure. T_{c} s are determined by the onset of diamagnetic transition or zero resistivity. In the doped samples, the T_{c} and a -axis length values are those of the optimally-doped ones. $(\text{Sr},\text{La})\text{FBiS}_2$ has the longest a -axis among these compounds. In $RE(\text{O},\text{F})\text{BiS}_2$, a -axis shrinks and T_{c} increases with increasing atomic number of RE from La to Nd. The a -axis lengths of $\text{Bi}_2(\text{O},\text{F})\text{S}_2$ and $\text{Bi}_4\text{O}_4\text{S}_3$ / $\text{Bi}_3\text{O}_2\text{S}_3$, whose blocking layers contain fluorite-type BiO layers, are shorter than that of $Nd(\text{O},\text{F})\text{BiS}_2$, although ionic radius (coordination number 6)²⁷⁾ of Bi is between Nd and Pr. T_{c} s of BiS_2 -based superconductors under ambient pressure show a dome-like tendency with the top of $T_{\text{c}} \sim$ 5.5 K at $a \sim$ 3.98 Å in $(\text{Nd}_{0.2}\text{Sm}_{0.8})(\text{O}_{0.7}\text{F}_{0.3})\text{BiS}_2$ ²⁸⁾. When a -axis is longer than \sim 4.0 Å, significant increase of T_{c} is observed in HP resistivity measurement. In contrast, compounds with shorter a -axis lengths, $\text{Bi}_2(\text{O},\text{F})\text{S}_2$ and $\text{Bi}_4\text{O}_4\text{S}_3$, show rapid decrease of T_{c} in HP resistivity measurement.

The relation between lattice parameter and T_{c} for as-synthesized and HP annealed $\text{Bi}_2(\text{O},\text{F})\text{S}_2$ is summarized in **Fig. 6**. In the optimally-doped samples with a - and c -axes longer than \sim 3.97 Å and shorter than \sim 13.73 Å, the value of T_{c} is maintained at \sim 5.1 K. In the underdoped samples, a -axis is shorter than \sim 3.97 Å and c -axis is longer than \sim 13.73 Å, and T_{c} increases as a - and c -axis expands and shrinks by HP annealing. T_{c} s for undoped Bi_2OS_2 sintered under high pressures are also in this trend. It should be emphasized that in HP annealed / synthesized undoped Bi_2OS_2 , superconductivity is achieved without intentional carrier doping. In Bi_2OS_2 , the Bi-S planes are not very flat, the in-plane S-Bi-S angle being 159.8° ²⁵⁾. The expansion of a -axis may lead to flatter Bi-S plane. In LaOBiS_2 , F-doping not only increases the carrier concentration but also flattens the buckling of the Bi-S plane and this structural transformation is also related to the appearance of superconductivity²⁹⁾. Similar phenomena would happen in the undoped and underdoped $\text{Bi}_2(\text{O},\text{F})\text{S}_2$ by HP annealing, which resulted in the increases of T_{c} s in these samples.

The decrease of T_{c} in HP resistivity measurement might be explained by the tendency shown in **Fig. 6(a)**. In HP resistivity measurement, a -axis might shrink by applying high pressures at low temperatures, and superconductivity could be disappeared. Structural analysis on $\text{Bi}_2(\text{O},\text{F})\text{S}_2$ under high pressures at low temperatures would provide fruitful information to clear this point.

5. Conclusion

High pressure (HP) resistivity measurement and HP annealing were performed for a BiS₂-based superconductor Bi₂(O,F)S₂, which caused different variation of T_c . In HP resistivity measurement, T_c linearly decreased at the rate of -1.2 K GPa⁻¹. In contrast, by HP annealing at 2 GPa and 470°C, T_c increased in undoped and underdoped samples, and maintained at 5.1 K in optimally-doped sample.

In HP resistivity measurement high pressure is applied *in-situ* at low temperatures, while HP annealing quenches the high pressure and high temperature phase to ambient pressure. Although in both cases hydrostatic high pressure is applied to the sample by a cubic-anvil-type apparatus, the difference between the two methods should be considered carefully. HP annealing technique have been mainly developed on BiS₂-based superconductors, but this method can cause unique effects on physical properties of various layered compounds.

Acknowledgement

This work was partly supported by the JSPS KAKENHI Grant Number 26390045, and Izumi Science and Technology Foundation. We thank to Dr. T. Fujii and Dr. R. Toda at the Cryogenic Research Center of the University of Tokyo for their cooperation in resistivity measurement at ambient pressure.

*E-mail : tuogino@mail.ecc.u-tokyo.ac.jp

Reference

- 1) Y. Mizuguchi, H. Fujihisa, Y. Gotoh, K. Suzuki, H. Usui, K. Kuroki, S. Demura, Y. Takano, H. Izawa and O. Miura, Phys. Rev. B **86** 220510(R) (2012)
- 2) Y. Mizuguchi, S. Demura, K. Deguchi, Y. Takano, H. Fujihisa, Y. Gotoh, H. Izawa and O. Miura, J. Phys. Soc. Jpn **81** 114725 (2012)
- 3) J. Xing, S. Li, X. Ding, H. Yang and H.H. Wen, Phys. Rev. B **86** 214518 (2012)
- 4) R. Jha, A. Kumar, S. K .Singh and V. P. S.Awana, J. Sup. and Novel. Mag. **29** 499-502 (2013)
- 5) S. Demura, Y. Mizugichi K. Deguchi, H. Okazaki, H. Hara, T. Watanabe, S. J. Denholme, M. Fujioka, T. Ozaki, H. Fujihisa, Y. Gotoh, O. Miura, T. Yamaguchi, H. Takeya and Y. Takano, J. Phys. Soc. Jpn **82** 033708 (2013)
- 6) Xi Lin, X. Ni, B. Chen, X. Xu, X. Yang, J. Dai, Y. Li, X. Yang, Y. Luo, Q. Tao, G. Cao and Z. Xu, Phys. Rev. B **87** 020504(R) (2013)
- 7) H. F. Zhai, P. Zhang, S. Q. Wu, C. Y. He, Z. Tu Tang, H. Jiang, Y. L. Sun, J. K. Bao, I. Nowik, I. Felner, Y. W. Zeng, Y. K. Li, X. F. Xu, Q. Tao, Z. A. Xu, and G. H. Cao, *J. Am. Chem. Soc.* **136** (2014) 15386
- 8) Y. L. Sun, A. Ablimit, H. F. Zhai, J. K. Bao, Z. T. Tang, X. B. Wang, N. L. Wang, C. M. Feng and G. H. Cao, *Inorg Chem.* **53** 11125 (2014)
- 9) C. T. Wolowiec, D. Yazici, B. D. White, K. Huang, M. B. Maple, *Phys. Rev. B* **88** 064503

(2013)

- 10) T. Tomita, M. Ebata, H. Soeda, H. Takahashi, H. Fujihisa, Y. Gotoh, Y. Mizuguchi, H. Izawa, O. Miura, S. Demura, K. Deguchi and Y. Takano J. Phys. Soc. Jpn **83** 063704 (2014)
- 11) C. T. Wolowiec, B. D. White, I. Jeon, D. Yazici, K. Huang, M. B. Maple, J. Phys.: Condens. Matter **25** (2013) 422201
- 12) R. Jha, B. Tiwari and V. P. S. Awana, J. Phys. Soc. Jpn **83** 063707
- 13) Y. Luo, H. F. Zhai, P. Zhang, Z. A. Xu, G. H. Cao and J. D. Thompson, Phys. Rev. B **90** 220510(R) (2014)
- 14) S. Demura, K. Deguchi, Y. Mizuguchi, K. Sato, R. Honjyo, A. Yamashita, T. Yamaki, H. Hara, T. Watanabe, S. J. Denholme, M. Fujioka, H. Okazaki, T. Ozaki, O. Miura, T. Yamaguchi, H. Takeya and Y. Takano, arXiv:1311.4267
- 15) J. Kajitani, K. Deguchi, T. Hiroi, A. Omachi, S. Demura, Y. Takano, O. Miura and Y. Mizuguchi, J. Phys. Soc. Jpn **83** 065002 (2014)
- 16) J. Kajitani, K. Deguchi, A. Omachi, T. Hiroi, Y. Takano, H. Takatsu, H. Kadowaki, O. Miura and Y. Mizuguchi, Solid State Comunn. **181** 1 (2014)
- 17) T. Okada, H. Ogino, J. Shimoyama and K. Kishio, Appl. Phys. Express **8** 023102 (2015)
- 18) J. Shao, X. Yao, Z. Liu, L. Pi, S. Tan, C. Zhang, and Y. Zhang, Supercond. Sci. Technol. **28** 015008 (2015)
- 19) N. Mori, H. Takahashi and N. Takeshita, High Pressure Research, **24** 225-232 (2004)
- 20) N. Shirakawa and M. Tamura, Polyhedron, **24** 2405-2408 (2005)
- 21) M. A. Il'ina, Sov. Phys. Solid State, **18** 1051-1055 (1976)
- 22) M. A. Il'ina, E. S. Itskevich and E. M. Dizhur, Sov. Phys. JETP 34(6) 1263-1265 (1972)
- 23) H. Kotegawa, Y. Tomita, H. Tou, H. Izawa, Y. Mizuguchi, O. Miura, S. Demura, K. Deguchi and Y. Takano J. Phys. Soc. Jpn. **81**.103702 (2012)
- 24) L. Li, D. Parker, P. Babkevich, L. Yang, H. M. Ronnow, and A. S. Sefat, arXiv : 1412.3070
- 25) W. A. Phelan, D. C. Wallace, K. E. Arpino, J. R. Neilson, K. J. Livi, C. R. Seabourne, A. J. Scott and T. M. McQueen, J. Am. Chem. Soc., **135** 5372 (2013)
- 26) Y. Mizuguchi, Physics Procedia 58, 94 (2014)
- 27) R. D. Shannon and C. T. Prewitt, Acta. Cryst. B25, 925 (1969)
- 28) J. Kajitani, T. Hiroi, A. Omachi, O. Miura and Y. Mizuguchi, arXiv: 1408.2625
- 29) A. Miura, M. Nagao, T. Takei, S. Watauchi, I. Tanaka and N. Kumada, J. Solid State Chem. 212 213 (2014)

Figure Captions

Figure 1. Temperature dependence of resistivity under high pressures for the optimally-doped $\text{Bi}_2(\text{O},\text{F})\text{S}_2$.

Figure 2. P - T phase diagram for optimally-doped $\text{Bi}_2(\text{O},\text{F})\text{S}_2$. T_c for Bi(III) and Bi(V) are cited from Ref. 21 and 22.

Figure 3. (a) XRD patterns and (b) Temperature dependence of magnetizations for $\text{Bi}_2(\text{O}_{1-x}\text{F}_x)\text{S}_2$ before and after HP annealing

Figure 4. (a) XRD patterns and (b) Temperature dependence of magnetizations for undoped Bi_2OS_2 sintered at ambient and high pressures

Figure 5. T_c s on various BiS_2 -based superconductors at ambient pressure and at ~ 2 GPa as a function of a -axis length at ambient pressure

Figure 6. The relationship between lattice parameter and T_c of $\text{Bi}_2(\text{O},\text{F})\text{S}_2$.

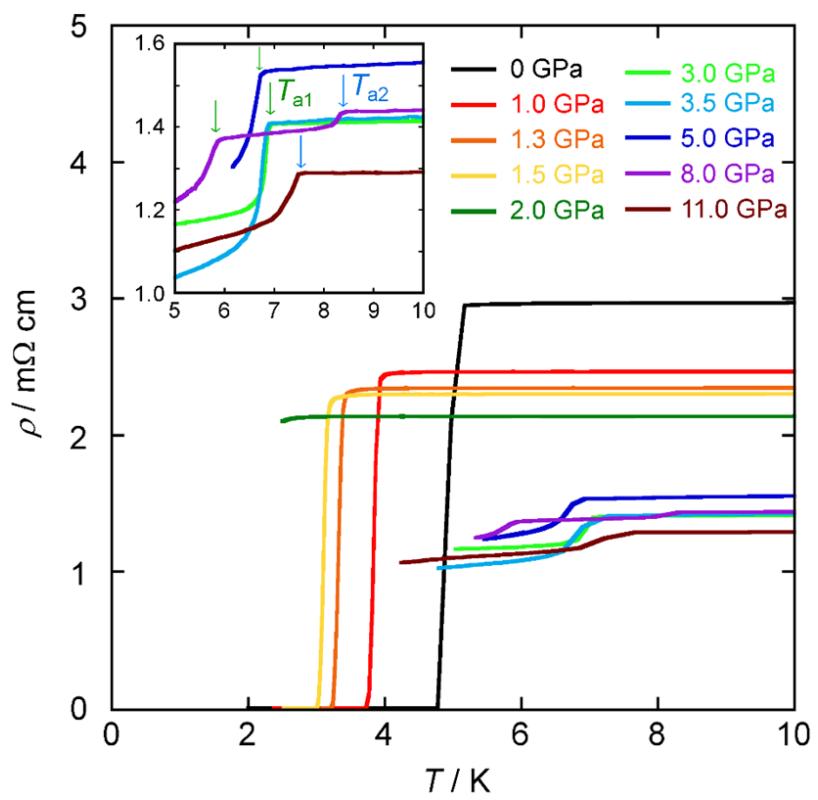


Figure 1.

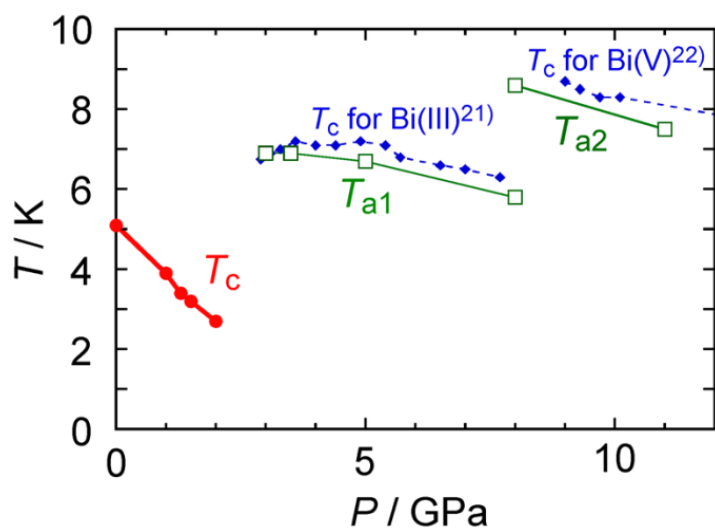


Figure 2.

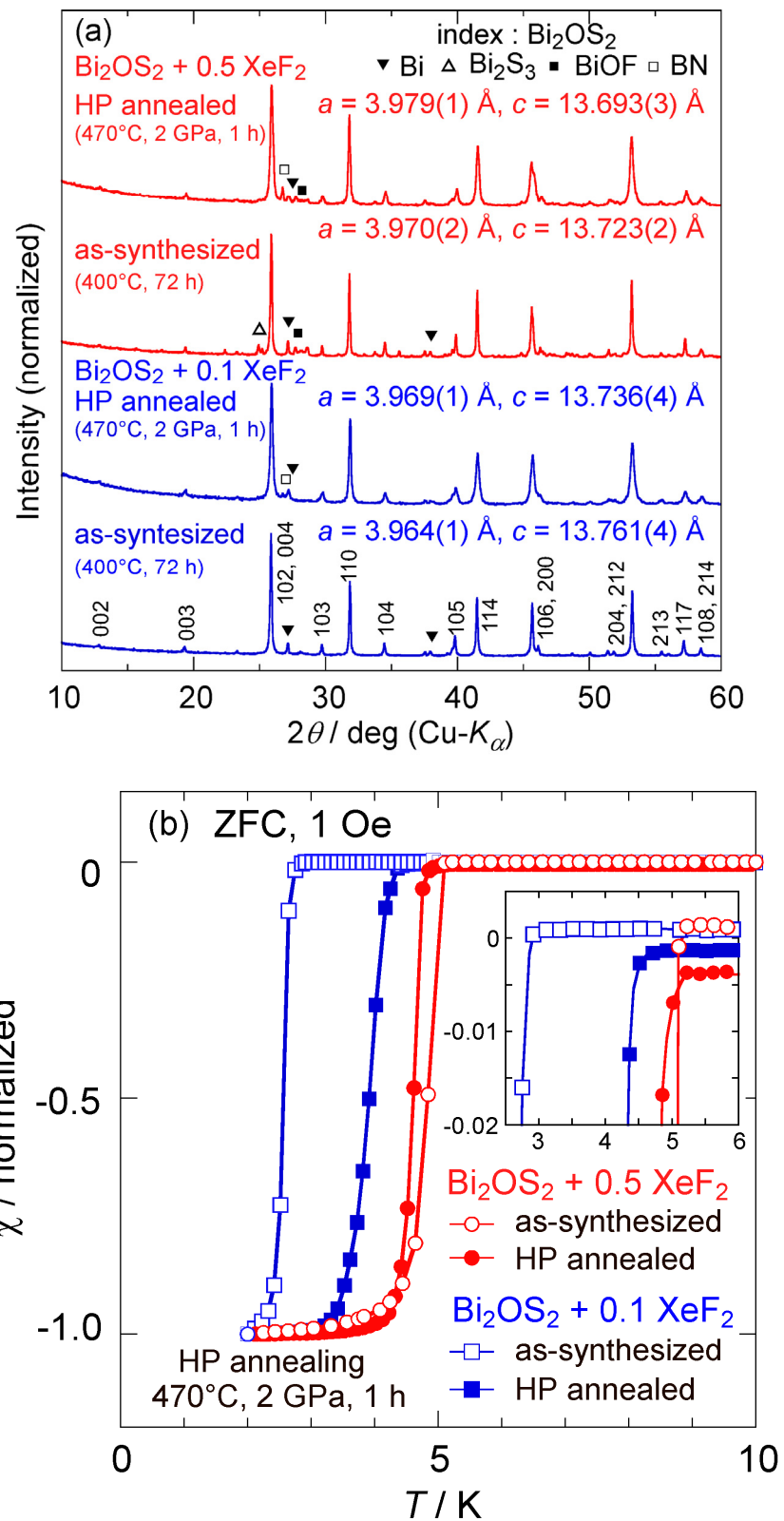


Figure 3.

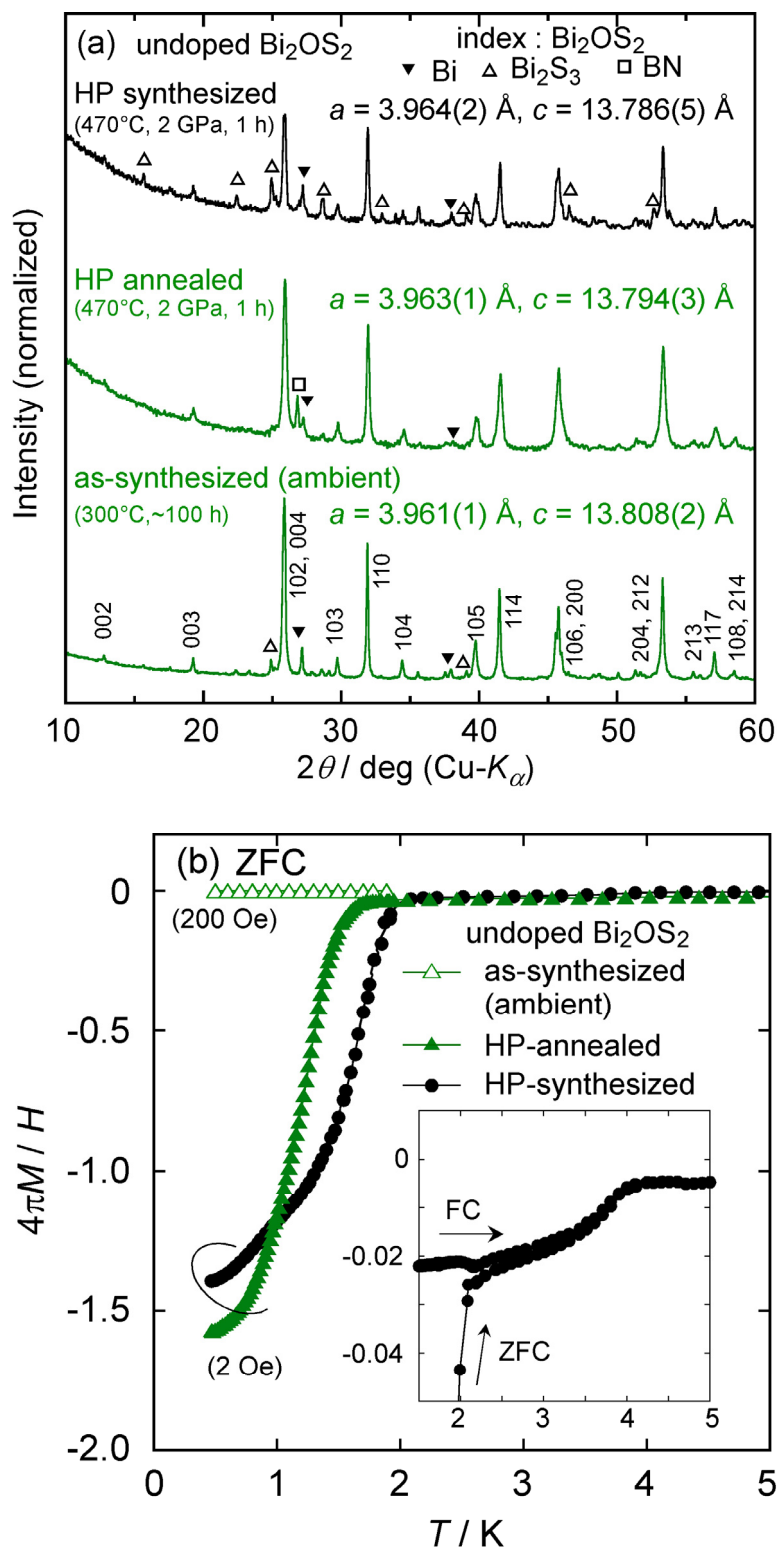


Figure 4.

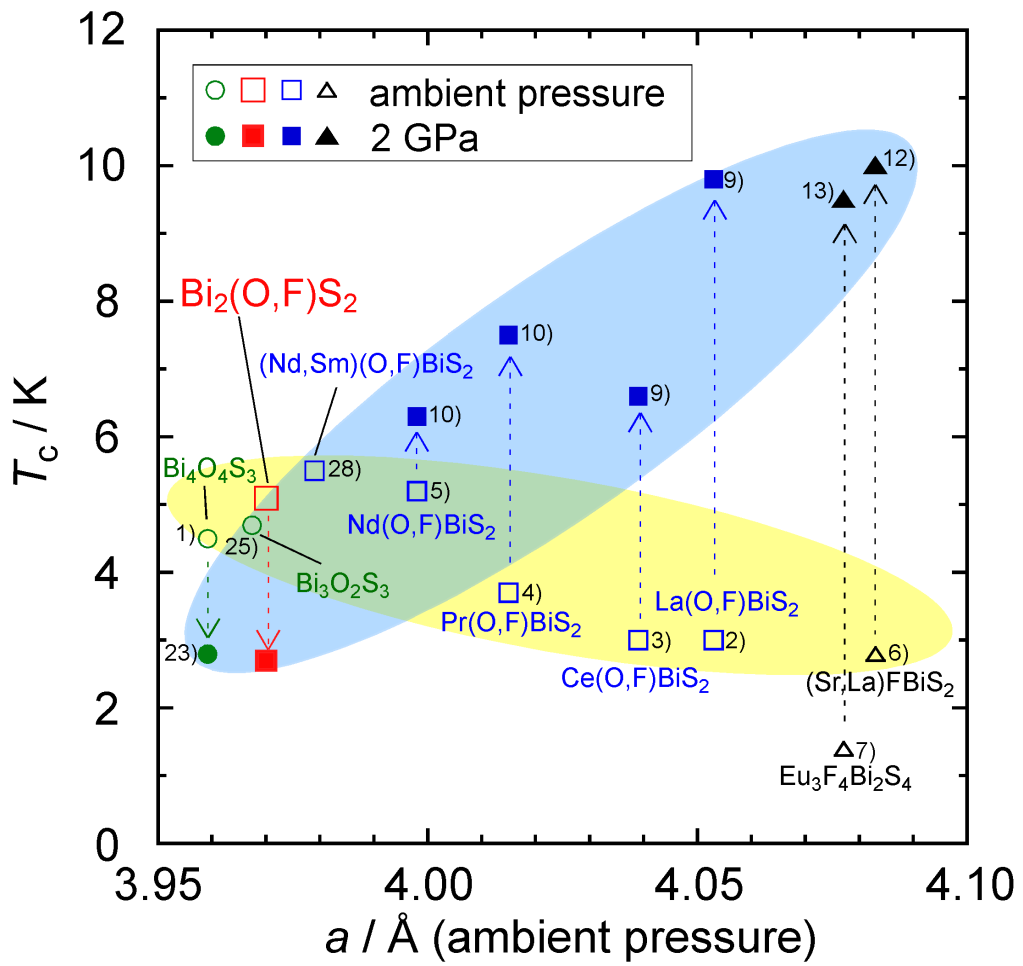


Figure 5.

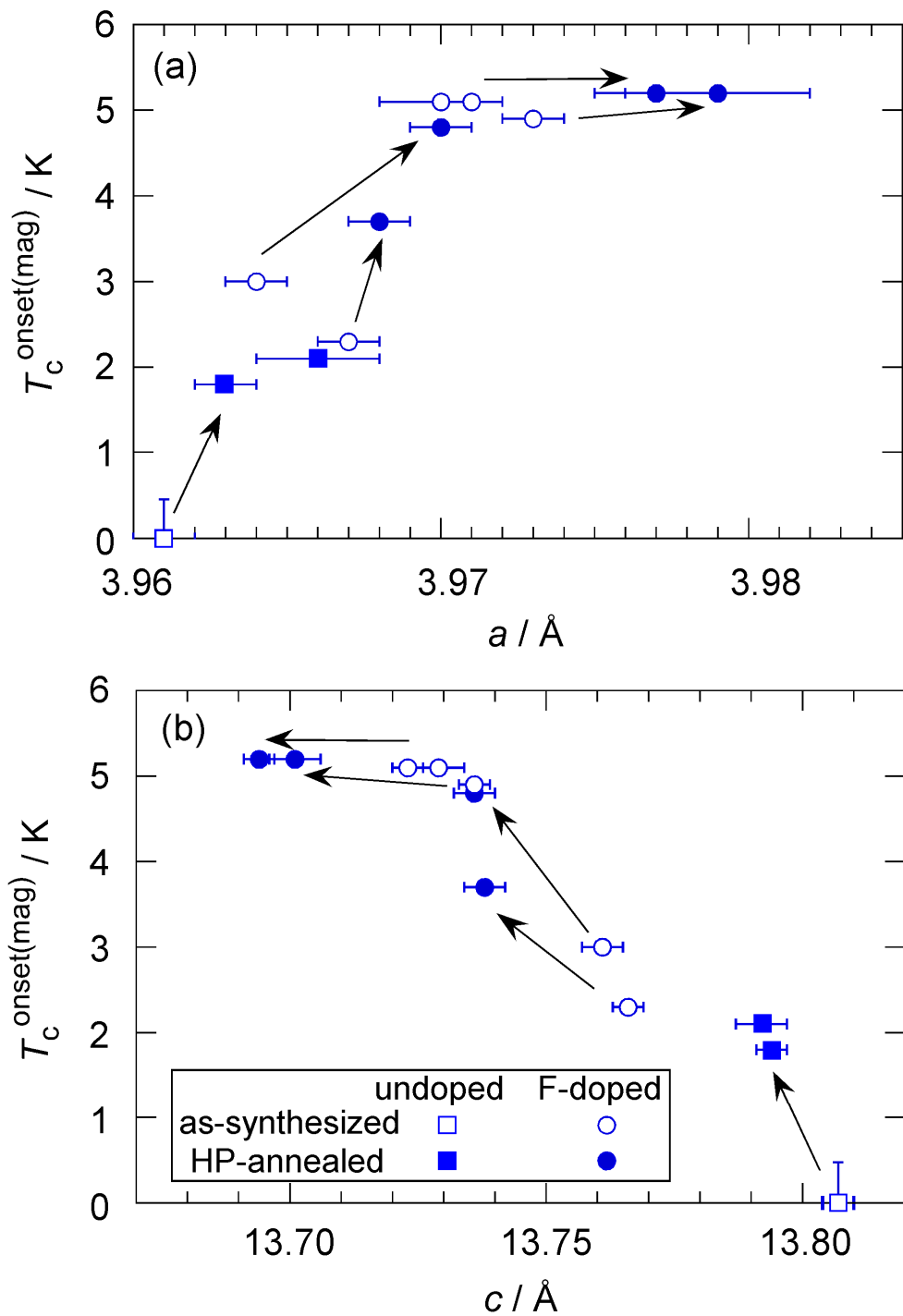


Figure 6.